

GLAD: Generative Language-Assisted Visual Tracking for Low-Semantic Templates

Xingyu Luo^{1†}, Yidong Cai^{1†}, Jie Liu^{1*}, Jie Tang¹, Gangshan Wu¹, Limin Wang¹

¹State Key Laboratory for Novel Software Technology, Nanjing University, Nanjing, 210023, China.

*Corresponding author(s). E-mail(s): liujie@nju.edu.cn;

Contributing authors: 652025330020@mail.nju.edu.cn; dawnyc1123@gmail.com; tangjie@nju.edu.cn; gswu@nju.edu.cn; lmwang@nju.edu.cn;

†These authors contributed equally to this work.

Abstract

Vision-language tracking has gained increasing attention in many scenarios. This task simultaneously deals with visual and linguistic information to localize objects in videos. Despite its growing utility, the development of vision-language tracking methods remains in its early stage. Current vision-language trackers usually employ Transformer architectures for interactive integration of template, search, and text features. However, persistent challenges about low-semantic images including prevalent image blurriness, low resolution and so on, may compromise model performance through degraded cross-modal understanding. To solve this problem, language assistance is usually used to deal with the obstacles posed by low-semantic images. However, due to the existing gap between current textual and visual features, direct concatenation and fusion of these features may have limited effectiveness. To address these challenges, we introduce a pioneering **G**enerative **L**anguage-**A**ssiste**D** tracking model, **GLAD**, which utilizes diffusion models for the generative multi-modal fusion of text description and template image to bolster compatibility between language and image and enhance template image semantic information. Our approach demonstrates notable improvements over the existing fusion paradigms. Blurry and semantically ambiguous template images can be restored to improve multi-modal features in the generative fusion paradigm. Experiments show that our method establishes a new state-of-the-art on multiple benchmarks and achieves an impressive inference speed. The code and models will be released at: <https://github.com/Confetti-lxy/GLAD>

Keywords: Deep Learning, Vision Language Tracking, Diffusion Model, Low-Quality Template

1 Introduction

Vision-language tracking task (Feng et al. 2021; Wang et al. 2021a; Zhou et al. 2023; Guo et al. 2022) has gradually enabled various applications in daily life scenarios. This task usually requires descriptive (Zheng et al. 2023) information from

both the vision and language modality of the target object. Vision-language trackers will generate a bounding box prediction as the output on each video frame. Considering that natural language can provide clear semantic information (Yang et al. 2019; Huang et al. 2021) while visual templates can

depict the textural information (Cui et al. 2022; Ye et al. 2022), unification of these two kinds of descriptive information will help reduce the ambiguity during tracking and finally assist the tracker to recognize the target. Unfortunately, research on vision-language tracking remains limited at present, particularly in scenarios involving low-semantic images.

Up to the present moment, for the traditional visual tracking task (Bertinetto et al. 2016; Bhat et al. 2018; Danelljan et al. 2019; Song et al. 2018; Wang et al. 2021b; Chen et al. 2023b; Wei et al. 2023), the descriptive information is usually a template image which contains the target object. Meanwhile, the tracking by natural language specification” (Li et al. 2017; Feng et al. 2020) attempts to locate the template only by the text initialization and then construct their pipeline similar to visual tracking. Some vision-language trackers (Guo et al. 2022; Zhou et al. 2023) borrow ideas from natural language tracking methods to perform separate processing on texts and then perform integration with visual features for enhancement.

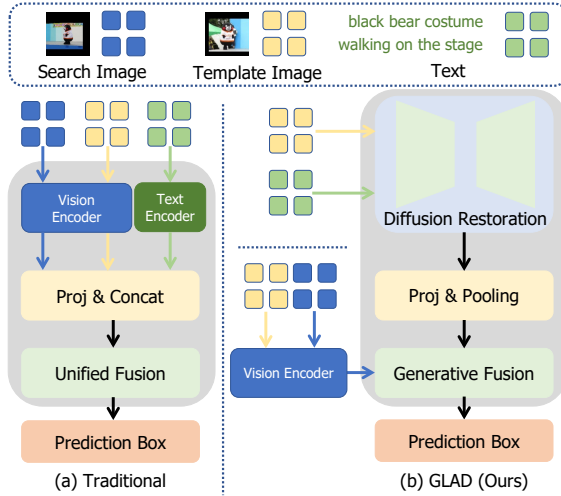


Fig. 1: Paradigms for Vision-Language trackers. The top section shows the inputs, including text, search image, and template image. (a) Traditional paradigm on the left directly concatenates different features and conducts a simple unified fusion. (b) Our generative paradigm on the right employs diffusion models for restoration of suboptimal template images, and interactions with original images are then conducted during generative fusion.

The classical vision-language trackers, as shown on the left half of Figure 1, mainly extract features from different modalities based on separate networks. Generally, text features are extracted by text models such as BERT (Devlin et al. 2018) and GPT (Brown et al. 2020), while image features, including template and search features, are extracted in a siamese way from image models such as ResNet (He et al. 2016) and ViT (Dosovitskiy et al. 2020). After that, different multi-modal fusion schemas will be taken to enhance image features with text features in different paradigms.

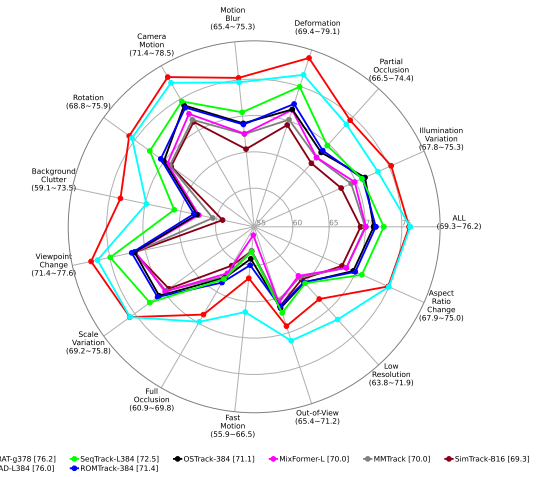


Fig. 2: Radar plot of AUC scores for LaSOT attributes, including Motion Blur, Camera Motion, Deformation, Illumination Variation, Out-of-View, Scale Variation, and Background Clutter. The figure illustrates the tracking performance of different models under diverse challenging conditions. A larger enclosed area indicates better overall tracking performance across all attribute types.

However, these paradigms extract text features and send them directly into fusion stage, connections between text and visual representations are not sufficiently considered for this task. In cases of low-semantic templates, which we consider from the low clarity of the tracking target and the weak relevance to the text description, feature fusion is further hindered, which adversely affects the prediction results and leads to poor performance. Besides, the inherent limitations of existing vision-language tracking models, which are predominantly discriminative in nature, relying on feature interaction

between the text, template, and search region to generate the final bounding box. As a result, these models typically lack the generative capability to reconstruct or enhance input data.

In light of these challenges, we propose the generative fusion paradigm shown on the right half of Figure 1, which focuses on leveraging a generative fusion to bolster compatibility between language and image. In contrast of discriminative models, generative models like Stable Diffusion possess stronger reconstruction abilities and can produce features during the generation process that are otherwise inaccessible to discriminative approaches. These features can act as a form of guidance, helping the model better understand and locate the target object. Specifically, text and template features are fused in a generative schema, enhancing the semantic fusion process to improve the semantic richness of low-semantic templates (visualized in Section 4.6.1). Compared with existing paradigms, our paradigm prevents semantic mismatches between texts and search images, restores the template and substitutes the process by interaction with diffusion features. Diffusion features are more robust because the generative fusion process augments details of the target in template features with the help of texts, thus promoting the relation modeling process.

Based on this paradigm, we propose a new vision-language tracking method GLAD, which employs diffusion models to perform generative multi-modal fusion. Verified by experiments, our method surpasses most existing state-of-the-art vision-language trackers in terms of both tracking accuracy and inference speed on LaSOT (Fan et al. 2019), LaSOT_{ext} (Fan et al. 2021), TNL2K (Wang et al. 2021a) and OTB99-lang (Li et al. 2017). In particular, our method exhibits significant advantages in the attributes of background clutter and deformation, showcasing a superior discriminative ability of the model, which is shown in Figure 2.

In general, our contributions are three-folds: (1) We propose a new generative paradigm for vision-language tracking which augments template features with the help of text, offering a novel perspective to the field. (2) Building upon this paradigm, we propose a new vision-language tracking framework named GLAD, which can effectively restore low-semantic templates. (3) Our GLAD-L384 model achieves state-of-the-art results on several vision-language tracking datasets and also

surpasses many vision-only models, maintaining an impressive inference speed of 44 FPS.

2 Related Work

2.1 Vision-Language Tracking

The core of the vision-language tracking task (Li et al. 2017; Feng et al. 2020; Yang et al. 2020; Li et al. 2022; Guo et al. 2022; Shao et al. 2024) lies in effectively leveraging both visual and textual cues of a specific target to achieve accurate localization in a given video sequence. Compared to traditional vision-only trackers, which rely solely on appearance information extracted from image sequences, vision-language trackers introduce additional semantic guidance from natural language descriptions. This allows the model to better distinguish between visually similar objects and to remain robust under challenging scenarios such as occlusion, illumination variation, and background clutter. In this setting, the textual description provides a complementary semantic reference for the visual features, thereby serving as a high-level constraint that helps disambiguate the target. As a result, the central challenge of vision-language tracking becomes how to conduct effective and interpretable multi-modal fusion between visual and linguistic representations.

Most existing solutions (Feng et al. 2021; Wang et al. 2021a) employ pre-trained language encoders such as BERT (Devlin et al. 2018) and GPT (Brown et al. 2020) to embed textual features into vectorized tokens. These token embeddings are then incorporated into visual features through attention mechanisms or feature modulation strategies, enabling interaction between the two modalities. Transformer-based architectures (Vaswani et al. 2017) have become the mainstream framework for such multi-modal fusion due to their strong capacity for contextual reasoning. Representative examples include TransVLT (Zhao et al. 2023), which employs a cross-attention mechanism to align visual and linguistic embeddings, and JointNLT (Zhou et al. 2023), which jointly models target grounding and tracking through a unified Transformer framework.

Since the current multi-modal fusion design is naive and inflexible, we propose a novel generative multi-modal fusion schema to solve the problem.

2.2 Diffusion Model

Diffusion models (Ho et al. 2020; Sohl-Dickstein et al. 2015; Song and Ermon 2019; Song et al. 2020; Lugmayr et al. 2022) have emerged as the new state-of-the-art family of generative models in computer vision. The key idea of diffusion models like DDPMs (Ho et al. 2020; Sohl-Dickstein et al. 2015), SGMs (Song and Ermon 2019, 2020) and Score SDEs (Karras et al. 2022; Song et al. 2021, 2020) is to progressively perform denoising process on noised data. For example, DDPM mainly uses two Markov chains: a forward chain that adds noise to images and a reverse chain that converts noised data back to images.

With the advancement of large-scale vision-language models, diffusion models have been further extended to cross-modality generation tasks, as exemplified by Stable Diffusion (Rombach et al. 2022) and DALLE 2 (Rassin et al. 2022). These approaches enable the generation of high-fidelity visual content conditioned on textual prompts, greatly promoting the development of Artificial Intelligence Generated Content (AIGC). Inspired by their powerful generative capability, many subsequent works have explored diffusion-based architectures for image restoration tasks, focusing on reconstructing fine-grained textures and recovering degraded visual details, which in turn enhance the perceptual realism and semantic consistency of the restored images. (Li et al. 2025; Zhao et al. 2020) Such improvements in image quality not only lead to visually pleasing results but also provide more reliable and semantically complete representations. (Russakovsky et al. 2015; Quan et al. 2024)

Recently, many other methods, such as efficient sampling and improved likelihood, have been applied to diffusion models to improve inference speed. Furthermore, some studies (Chen et al. 2023a; Pvnr et al. 2023) have demonstrated that the appropriate integration of generative diffusion models into the denoising process can provide auxiliary structural and semantic cues, thereby benefiting a range of downstream vision tasks (Cheng et al. 2025) such as object detection (Ge et al. 2025) and ultimately enhancing the representational capacity and robustness of visual models. Building on this insight, we propose a generative multimodal fusion schema that incorporates diffusion-based

features into the tracking process, aiming to overcome the rigidity of current discriminative fusion designs.

3 Method

For the tracking task, the model needs to determine the target’s position in each search frame based on both the template image and the accompanying text description. Although the template provides essential visual cues, it often lacks sufficient semantic information, which increases the difficulty of distinguishing the target in cluttered or ambiguous scenes. To compensate for this limitation, textual descriptions are introduced to supply richer semantic context and guide the tracking process. Nevertheless, due to the inherent semantic gap between textual and visual representations, directly incorporating language features into visual pipelines usually provides only limited improvements, especially when the visual template itself is of low quality or poorly aligned with the textual description.

Therefore, we intend to use a diffusion model to leverage text information for template restoration and obtain a highly semantic fused feature, thereby enhancing the performance of vision-language trackers. As a result, we introduce diffusion model in our method that employs text to guide and rectify the template.

Figure 3a shows the overall framework of GLAD, including three main components: the Generative Diffusion Module, the cascaded Multi-Modal Decoders (N in total, each consists of one attention pooling module and one feature decoding module), and the Head used to predict the final coordinate.

3.1 Generative Diffusion Module

Due to the inherent semantic gap between textual and visual features, traditional fusion paradigms that directly combine text and template representations often fail to make full use of the semantic richness of language, treating textual cues as auxiliary signals rather than deeply integrated guidance. This limitation is particularly evident in discriminative models, which mainly rely on feature interaction without the capacity to reconstruct or refine the target representation. In contrast, generative diffusion models have

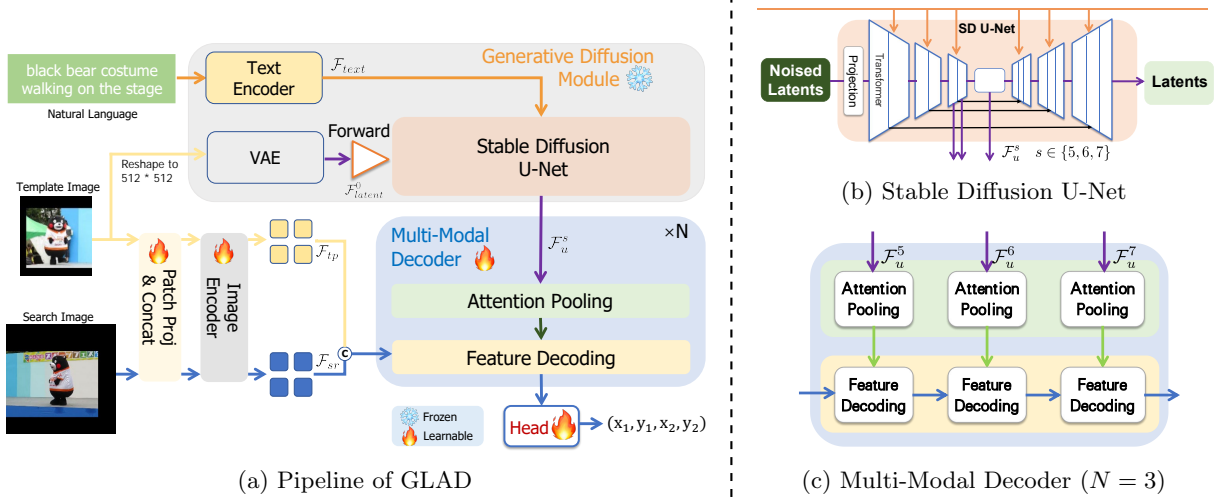


Fig. 3: Pipeline of the proposed GLAD model. (a) Firstly, the natural language and the template image will be generatively fused using the Generative Diffusion Module. Secondly, the generated diffusion features are passed through the cascaded Multi-Modal Decoder to enhance semantic information. Search features are concatenated with template features for decoding modules under the guidance of the fused features from pooling modules. (b) Details of Stable Diffusion U-Net. (c) Details of Multi-Modal Decoder ($N = 3$).

recently demonstrated remarkable success in both image generation and video understanding, showing their ability to capture fine-grained semantics and structural details during the denoising process. Such generative capabilities offer a promising new approach for enhancing template quality and bridging the semantic gap in vision-language tracking.

By leveraging the image-to-image capability of diffusion models, text descriptions and template images can be semantically combined to create high-quality template images and effectively utilize language information, which we refer to as template inpainting. This novel process will restore the template image and thus improve low-semantic template. Using the restored template from inpainting is unnecessary because we can simplify by leveraging intermediate features, whereby text and template features are fused to yield semantically richer multi-modal features. As shown in Figure 3b, the proposed method employs Stable Diffusion (SD) for generative fusion. It is based on the Latent Diffusion Model (LDM) (Song and Ermon 2019), which employs the similar of DDPM (Ho et al. 2020; Sohl-Dickstein et al. 2015) in latent space.

Specially, DDPM generally uses two Markov chains, the forward one to perturb data to noise and

the reverse one to remove this noise. For generating new data samples, DDPM starts by generating an unstructured noise vector from the prior distribution, then gradually removing noise by running a learnable Markov chain in the reverse process. Formally, DDPMs can be interpreted as a sequence of denoising autoencoders $\epsilon_\theta(x_t, t); t = 1, \dots, T$, which are trained to predict a denoised variant of their input x_t , where x_t is a noisy version of the input x . The corresponding objective can be simplified to:

$$L_{DDPM} = E_{x, \epsilon \sim \mathcal{N}(0, 1), t} [\|\epsilon - \epsilon_\theta(x_t, t)\|_2^2], \quad (1)$$

where E , \mathcal{N} denotes the normal distribution and t is uniformly sampled from $\{1, \dots, T\}$.

Compared to DDPM, LDM almost does the same thing, the difference is just that LDM needs to transform the high-dimensional pixel space into an efficient, low-dimensional latent space using the VAE (Kingma and Welling 2013; Rezende et al. 2014) encoder, where we will apply DDPM. The objective on the perceptually most relevant bits uses the reweighted bound, which now reads:

$$L_{LDM} = E_{\mathcal{E}(x), \epsilon \sim \mathcal{N}(0, 1), t} [\|\epsilon - \epsilon_\theta(z_t, t)\|_2^2]. \quad (2)$$

The neural backbone $\epsilon_\theta(\circ, t)$ of the diffusion model is implemented as a time-conditional U-Net (Dhariwal and Nichol 2021; Ho et al. 2020; Ronneberger et al. 2015; Song et al. 2020). Latent features of samples can also be decoded to image space using the VAE decoder.

In our GLAD pipeline, the U-Net from SD serves as the core architecture. It accepts noised latents and outputs denoised latents which are semantically restored. Template images are transferred to the latent space using VAE (Kingma and Welling 2013; Rezende et al. 2014), and then altered to noised latents through the forward process:

$$\begin{cases} \mathcal{F}_{latent} = \text{VAE}(template) \\ \mathcal{F}_{latent}^0 = \text{Forward}(\mathcal{F}_{latent}) \end{cases}, \quad (3)$$

where *template* represents the input template image and \mathcal{F}_{latent}^0 represents the noised latents.

As shown in Figure 3b, the U-Net structurally comprises two parts: the left contracting path and the right expanding path. The contracting path experiences a gradual decrease in resolution and increases in dimension, with the level of text information deepening, leading to progressively richer multi-modal semantic features. The expanding path, on the other hand, corresponds to an opposite upsampling process, with deep-layer features being used to recover shallow-layer information, thus aligning semantics more closely with the original latent representation. The U-Net in Figure 3b consists of 16 Transformer submodules, with 7 in the contracting path and 9 in the expanding path:

$$\begin{cases} \mathcal{F}_{text} = \text{TextEncoder}(text) \\ \mathcal{F}_u^s = \text{Transformer}_s(\mathcal{F}_{latent}^{s-1}, \mathcal{F}_{text}) \end{cases}, \quad (4)$$

where $s \in \{1, 2, 3, \dots, 16\}$ represents the sequence number of Transformer submodules and *text* represents the input natural language. Besides, \mathcal{F}_u^{16} represents the output denoised latents.

Aiming to fully exploit the deep semantic representations while still benefiting from shallower fusion cues and maintaining inference efficiency, we select three submodules from the contracting path of the U-Net, namely the 5-th, 6-th, and 7-th layers. The corresponding feature maps, denoted as \mathcal{F}_u^s ($s \in 5, 6, 7$), are then transferred to the Multi-Modal Decoder for further processing. These layers are chosen because they capture increasingly

abstract semantic information while retaining sufficient spatial structure, thus striking a balance between expressiveness and computational overhead. By incorporating the U-Net features in this manner, textual information can be more effectively integrated into the template, enabling the restoration of higher-quality target representations and alleviating the limitations of direct feature fusion.

Notably, this design does not amplify the discrepancy nor degrade performance, even when reshaping templates are used. This is because the template frame does not directly interact with the search image; instead, it is processed solely by the diffusion model, and only the resulting multimodal, target-centric semantic features are involved in the interaction, which prevents mismatches from affecting tracking performance.

As for the design choice of not directly feeding the generated template image into the backbone, while using the generated template image as input to the backbone could potentially enable stronger interaction with the search region (as shown by early-fusion designs like OTrack Ye et al. (2022)), we deliberately chose not to do so due to computational and inference efficiency concerns. The diffusion model already integrates the template and text semantics within the latent space and produces a rich fused representation. Decoding it into an image and then re-encoding it back into features via the backbone is both redundant and computationally expensive. Moreover, such a design would force the pipeline into serial execution—first generation, then tracking—thereby significantly limiting inference speed. To avoid this bottleneck, we directly use the fused features from the diffusion model and perform cross-attention fusion with the search region features after the backbone, balancing effectiveness and efficiency.

3.2 Multi-Modal Decoder

To solve the misalignment between features from Stable Diffusion U-Net and the image encoder, we propose a novel module for feature alignment and information fusion, which we name Multi-Modal Decoder. This module uses the multi-modal features fused within U-Net to assist the tracking process. Each Multi-Modal Decoder comprises one Attention Pooling Module and one Feature Decoding Module. There are N Multi-Modal Decoders

cascaded to sequentially exploit features from U-Net, where N equals the number of U-Net features. As shown in Figure 3b and Figure 3c, GLAD generally sets N to 3 for the balance of performance and efficiency.

3.2.1 Attention Pooling Module

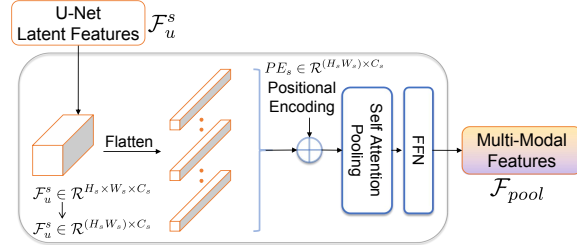


Fig. 4: Overview of the proposed Attention Pooling Module. It aligns the spatial and dimensional discrepancies between U-Net and visual encoder features while preserving semantic richness for effective multi-modal fusion.

Because the multi-modal features generated by the U-Net are inherently incompatible with the visual features extracted by the image encoder in terms of both spatial resolution and feature dimensionality, direct feature interaction becomes infeasible. To resolve this mismatch and simultaneously strengthen the semantic expressiveness of the fused representation, we propose an attention-based pooling module that performs dimension alignment while preserving semantic richness. As illustrated in Figure 4, features from the s -th Transformer submodule of the U-Net are first denoted as

$$\mathcal{F}_u^s \in \mathbb{R}^{H_s \times W_s \times C_s}, \quad (5)$$

where H_s and W_s represent the spatial height and width of the feature map, and C_s denotes the channel dimension. These features are subsequently flattened into a sequential representation for downstream processing,

$$\mathcal{F}_u^s \in \mathbb{R}^{(H_s W_s) \times C_s}. \quad (6)$$

Since this flattening operation inevitably discards the original spatial positional information, we introduce a learnable positional encoding to restore location awareness, defined as

$$PE_s \in \mathbb{R}^{(H_s W_s) \times C_s}. \quad (7)$$

At this stage, the multi-modal sequence enriched with positional encoding is expressed as

$$\mathcal{F}_m^s = \mathcal{F}_u^s + PE_s, \quad (8)$$

which restores the spatial location cues lost during flattening and prepares the features for further refinement.

This enriched representation \mathcal{F}_m^s then serves as the input to the subsequent self-attention pooling stage, where the features are not only semantically enhanced but also appropriately scaled and dimensionally aligned. In this way, the processed multi-modal features can be effectively integrated into the feature decoding module, ensuring both representational adequacy and compatibility for cross-modal fusion.

To be more specific, self-attention pooling operation conducts self-attention on the multi-modal features \mathcal{F}_m^s itself, promoting the fusion of global spatial information and reducing the feature dimensions to be suitable for the size of visual features. Here, we use q_m , k_m , and v_m as representations for query, key, and value embedding of \mathcal{F}_m^s in attention calculation. The calculation formula is:

$$Attn_m = \text{Softmax}\left(\frac{q_m k_m^T}{\sqrt{d}}\right) v_m. \quad (9)$$

Finally, a Feed Forward Network (FFN) is applied for output:

$$\mathcal{F}_{pool} = \text{FFN}(Attn_{tp}), \quad (10)$$

and the result \mathcal{F}_{pool} is then sent to the Feature Decoding Module for further semantic enhancement.

3.2.2 Feature Decoding Module

The Attention Pooling Module mainly ensures that the spatial resolution and feature dimensionality are aligned with those of the template features, thereby enabling cross-modal interaction. However, this step alone does not substantially enrich the semantic content of the search features, which remain relatively weak in expressive power. To overcome this limitation, we design a Feature Decoding Module that further leverages the multi-modal

features to strengthen their semantic representation and enhance their discriminative capacity for tracking, as illustrated in Figure 5.

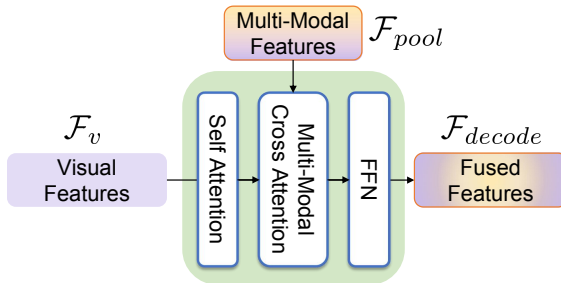


Fig. 5: Structure of the Feature Decoding Module. It enhances the semantic representation and discriminative ability of search features by leveraging multi-modal information from the Attention Pooling Module.

In the Feature Decoding Module, the visual features are constructed as the concatenation of template features and search features, formally defined as

$$\mathcal{F}_{tp} = \text{Enc}(I_{tp}), \quad \mathcal{F}_{sr} = \text{Enc}(I_{sr}), \quad (11)$$

where I_{tp} and I_{sr} denote the template image and the search region image, respectively, and $\text{Enc}(\cdot)$ represents the Image Encoder (Ye et al. 2022). The combined visual feature representation is then given by

$$\mathcal{F}_v = \text{Concat}(\mathcal{F}_{tp}, \mathcal{F}_{sr}). \quad (12)$$

This concatenated representation allows the model to jointly consider information from both the template and the search region within a unified feature space. To capture long-range dependencies and global spatial relationships, we apply a self-attention mechanism over the visual features \mathcal{F}_v . Specifically, if we denote the concatenated embeddings as query, key, and value matrices q_v , k_v , and v_v , the output of the self-attention layer is computed as

$$\text{Output}_{SA} = \text{Softmax} \left(\frac{q_v k_v^T}{\sqrt{d}} \right) v_v, \quad (13)$$

where d denotes the scaling factor corresponding to the feature dimension. This operation enables the model to adaptively reweight feature responses, ensuring that salient spatial patterns across the template and search regions are effectively emphasized in the decoding process.

Then, the multi-modal features from the Attention Pooling Module, denoted as \mathcal{F}_{pool} , are introduced into the cross-attention operation. Specifically, \mathcal{F}_{pool} is linearly projected to obtain the key and value matrices:

$$k_{pool} = W_k \mathcal{F}_{pool}, \quad v_{pool} = W_v \mathcal{F}_{pool}, \quad (14)$$

where W_k and W_v are learnable projection matrices. Meanwhile, the query embeddings are derived from the output of the self-attention layer, expressed as

$$q_v = W_q \text{Output}_{SA}, \quad (15)$$

with W_q representing the projection matrix for query embeddings. The cross-attention output is then calculated as

$$\text{Output}_{CA} = \text{Softmax} \left(\frac{q_v k_{pool}^T}{\sqrt{d}} \right) v_{pool}, \quad (16)$$

where d denotes the scaling factor corresponding to the feature dimension. Finally, a Feed-Forward Network (FFN) is applied channel-wise to the attended features for consolidation, yielding the decoded representation

$$\mathcal{F}_{decode} = \text{FFN}(\text{Output}_{CA}), \quad (17)$$

which is subsequently forwarded to the Head Network for target location prediction.

3.3 Head

The head module is responsible for predicting the key points of target bounding boxes. In prior works, this component is often implemented either through a Multi-Layer Perceptron (MLP) or a corner-based fully Convolutional Neural Network (CNN). However, visualization analyses from Mix-Former (Cui et al. 2022) reveal that corner-based designs negatively impact the capability of relation modeling modules, as they force the network

to attend disproportionately to local boundaries rather than capturing holistic object cues. To mitigate this limitation, we adopt a center-based design, which encourages the network to concentrate on the central position of the target and improves the robustness of bounding box regression.

Specifically, we employ a fully convolutional center-based localization head (Zhou et al. 2019) to estimate the bounding boxes of tracked objects. The head consists of L stacked Conv-BN-ReLU layers, which progressively refine the feature representation for accurate localization. Specifically, the head outputs three types of prediction maps:

$$C \in [0, 1]^{H_{sr} \times W_{sr}}, \quad (18)$$

$$O \in [0, 1]^{2 \times H_{sr} \times W_{sr}}, \quad (19)$$

$$S \in [0, 1]^{2 \times H_{sr} \times W_{sr}}, \quad (20)$$

where C denotes the classification score map, O represents the local offset map, and S indicates the normalized bounding box size map. Here, H_{sr} and W_{sr} refer to the spatial resolution of the search image, while P is the patch size used in feature extraction.

Finally, the position corresponding to the maximum classification score in C is selected as the predicted target center. The target bounding box is then obtained by combining this position with the offset and size information provided by O and S , respectively. Formally, if (x_c, y_c) denotes the predicted center location, the bounding box can be expressed as

$$B = (x_c + O_x, y_c + O_y, S_w, S_h), \quad (21)$$

where (O_x, O_y) are the local offsets from the offset map O , and (S_w, S_h) are the predicted width and height of the bounding box from the size map S .

3.4 Optimization for Efficiency

The native Stable Diffusion¹ model encounters problems with inference efficiency in image generation, mainly resulting from a large number

of denoising steps. It poses significantly negative impacts on training and inference for the proposed GLAD method. To solve this problem, GLAD applies a technique that can accelerate the denoising speed of diffusion models, called Latent Consistency Model (LCM) (Luo et al. 2023), to optimize the efficiency of the generative multi-modal fusion process.

Inspired by Consistency Models (CM) (Song et al. 2023), this technique integrates the principles of Latent Diffusion Models (LDM) (Rombach et al. 2022) to design a Latent Consistency Model (LCM). It employs a distillation-based approach to finetune diffusion models, yielding a training-free acceleration plugin named LCM-LoRA (Luo et al. 2023). By combining the Stable Diffusion v1.5 model with the LCM-LoRA model, the denoising steps are reduced from the original 20 to 50 steps to only 2 to 8 steps, greatly enhancing the speed of the generative multi-modal fusion process and finally promoting efficiency in training and inference.

Through this approach, during inference, the diffusion process is applied only once at the first frame for initialization. Specifically, we adopt the SD-v1.5-inpainting model and perform a single denoising step, after which the fused features obtained are fixed and reused for subsequent tracking. In practical applications, the diffusion preparation time is relatively short—roughly comparable to the cost of a single-frame forward pass—making its impact on the overall inference latency negligible.

4 Experiment

4.1 Experimental Settings

GLAD is implemented using Python 3.8.18, Difusers 0.23.0, and PyTorch 2.1.1. The training process is conducted on 4 Nvidia Quadro RTX A6000 GPUs, while we use 1 Nvidia GeForce RTX 3090 GPU for inference and efficiency test. For the pretrained backbone, we adopt the widely used Stable Diffusion v1.5 model as the foundation for generative multi-modal fusion, owing to its strong text-to-image alignment capability and robust denoising performance. In addition, we employ the MAE-pretrained ViT (He et al. 2022) as the image encoder to provide high-quality visual representations. The Stable Diffusion v1.5

¹Stable Diffusion v1.5 is available at [huggingface - stable-diffusion-v1-5](https://huggingface.co/stable-diffusion-v1-5), a mirror of the deprecated ruwnayml repo.

Table 1: State-of-the-art Comparison on LaSOT, LaSOT_{ext}, TNL2K and OTB99-lang. The best two results are in **red** and **blue** fonts.

Method	LaSOT			LaSOT _{ext}		TNL2K			OTB99-lang	
	AUC(%)	$P_{Norm}(\%)$	P(%)	AUC(%)	P(%)	AUC(%)	$P_{Norm}(\%)$	P(%)	AUC(%)	P(%)
<i>Visual tracking method (vision-only)</i>										
DiMP (Bhat et al. 2019)	56.9	65.0	56.7	39.2	45.1	44.7	51.3	43.4	-	-
TransT (Chen et al. 2021)	64.9	73.8	69.0	45.1	51.2	50.7	57.1	51.7	-	-
MixViT (Cui et al. 2022)	69.6	79.9	75.9	-	-	-	-	-	-	-
MixFormerV2 (Cui et al. 2023)	70.6	80.8	76.2	50.6	56.9	57.4	-	58.4	-	-
OStrack (Ye et al. 2022)	69.1	78.7	75.2	47.4	53.3	54.3	-	-	-	-
SeqTrack-B256 (Chen et al. 2023b)	69.9	79.7	76.3	49.5	56.3	54.9	-	-	-	-
SeqTrack-L384 (Chen et al. 2023b)	72.5	81.5	79.3	50.7	57.5	57.8	-	-	-	-
SUTrack-L256 (Chen et al. 2025)	73.5	83.3	80.9	54.0	61.7	-	-	-	-	-
SUTrack-L256 (Chen et al. 2025)	75.2	84.9	83.2	53.6	60.5	-	-	-	-	-
ARTrack-B256 (Wei et al. 2023)	70.4	79.5	76.6	46.4	52.3	57.5	-	-	-	-
ARTrack-L384 (Wei et al. 2023)	73.1	82.2	80.3	52.8	59.7	60.3	-	-	-	-
<i>Vision-language tracking method</i>										
RTTNLD (Feng et al. 2020)	35.0	-	35.0	-	-	25.0	33.0	27.0	61.0	79.0
SNLT (Feng et al. 2021)	54.0	63.6	57.4	26.2	30.0	27.6	35.9	41.9	66.6	84.8
TNL2K-II (Wang et al. 2021a)	51.3	-	55.4	-	-	42.0	50.0	42.0	68.0	88.0
GTI (Yang et al. 2020)	47.8	-	47.6	-	-	-	-	-	58.1	73.2
Li et al. (Li et al. 2022)	53.0	56.0	-	-	-	44.0	52.0	45.0	69.0	91.0
VLT _{TT} (Guo et al. 2022)	67.3	-	72.1	48.4	55.9	53.1	-	53.3	76.4	93.1
TransVLT (Zhao et al. 2023)	66.4	-	70.8	-	-	56.0	61.7	-	69.9	90.6
JointNLT (Zhou et al. 2023)	60.4	69.4	63.6	-	-	56.9	73.6	58.1	65.3	85.6
QueryNLT (Shao et al. 2024)	59.9	69.6	63.5	-	-	57.8	75.6	58.7	66.7	88.2
MMTrack (Zheng et al. 2023)	70.0	82.3	75.7	49.4	55.3	58.6	75.2	59.4	70.5	91.8
DecoupleTNL (Ma and Wu 2023)	64.9	-	67.1	-	-	40.7	-	40.0	69.5	92.8
All-in-one (Zhang et al. 2023)	71.7	82.4	78.5	54.5	62.0	55.3	-	57.2	71.0	93.0
ChatTracker (Sun et al. 2024)	71.7	80.9	77.5	-	-	59.6	76.3	62.1	-	-
DMTrack-256 (Zhang et al. 2024)	66.8	-	72.7	47.3	52.1	57.7	-	59.9	69.3	90.9
DMTrack-384 (Zhang et al. 2024)	70.1	-	76.5	51.1	58.3	61.6	-	65.4	71.2	92.3
GLAD-B256 (Ours)	69.5	79.6	74.2	50.6	55.7	59.7	77.6	62.2	69.6	92.4
GLAD-L384 (Ours)	76.0	86.8	85.1	55.9	64.6	62.1	80.4	66.2	71.4	93.2

model contains the Text Encoder, the Variational Autoencoder (VAE), the Forward process, and the U-Net, which collectively support multi-modal representation learning. On top of this architecture, we design three attention pooling modules and three feature decoding modules in the Multi-Modal Decoder, both of which are initialized with the Xavier scheme (Glorot and Bengio 2010) to stabilize training and accelerate convergence.

For GLAD-Base, the input resolution of the search image is set to 256×256 , while for GLAD-Large, the resolution is increased to 384×384 , providing higher spatial fidelity for more challenging tracking scenarios. Similarly, the template image is configured with a resolution of 128×128 in GLAD-Base and 192×192 in GLAD-Large, ensuring a balanced trade-off between computational

efficiency and representational quality. In order to align with the requirements of the Stable Diffusion v1.5 backbone, the template images from both variants are further reshaped to 512×512 during the template inpainting stage, which guarantees consistency with the generative module and preserves the semantic richness of reconstructed features.

For the training stage, we include the training splits of GOT-10k (Huang et al. 2019), LaSOT (Fan et al. 2019), OTB99-lang (Li et al. 2017), TNL2K (Wang et al. 2021a), TrackingNet(Muller et al. 2018), RefCOCOg (Mao et al. 2016) to train our model. The whole training process takes 300 epochs, using AdamW(Loshchilov and Hutter 2017) optimizer with weight decay of 10^{-4} and gradient clipping of 0.1. Besides, we employ a compound loss function that combines L1

loss, to enforce precise coordinate regression, and GIoU loss as follows, to enhance spatial alignment and robustness in bounding box prediction.

$$L_{loc} = \lambda_{L1} L_1(B_i, \hat{B}_i) + \lambda_{giou} L_{giou}(B_i, \hat{B}_i), \quad (22)$$

where $\lambda_{L1} = 5$ and $\lambda_{giou} = 2$ are the weights of the two losses, B_i is the ground-truth bounding box and \hat{B}_i is the predicted bounding box of the targets.

During training, the warm-up strategy is adopted. The learning rate first increases to 4×10^{-4} linearly at the first 30 epochs and then drops to 4×10^{-5} after 240 epochs. For GLAD, pretraining is necessary for Image Encoder. We pretrain the Image Encoder with the Visual Object Tracking task to get an appropriate initialization for the Vision-Language Tracking task. Moreover, we adopt the DeepSpeed(Rasley et al. 2020) ZeRO(Rajbhandari et al. 2020) Stage 2 strategy during training. This strategy partitions the optimizer states and gradients into parallel workflows for each device, significantly reducing the GPU memory consumption during training and improving the training speed.

While for the evaluate stage, we evaluate our model for vision-language tracking on the mainstream tracking benchmarks with natural language descriptions, including LaSOT (Fan et al. 2019), TNL2K (Wang et al. 2021a), OTB99 (Li et al. 2017) and LaSOT_{ext} (Fan et al. 2021). Besides, we also evaluate our model on the traditional visual tracking dataset GOT-10k (Huang et al. 2019) to verify the tracking performance in a vision-only scenario. We generally follow the convention (Chen et al. 2021; Ye et al. 2022; Zhang et al. 2020) by applying a simple Hanning window penalty to the output of the head network to utilize positional prior information. For acceleration techniques, we only used FP16 precision and Flash Attention, both of which are commonly adopted acceleration strategies.

4.2 Comparison with the State-of-the-art Methods

This section demonstrates the performance of GLAD on various visual language tracking datasets and compares it with current mainstream methods, which is shown in Table 1. Compared to vision-language trackers, GLAD-L384 establishes a new SOTA on LaSOT (Fan et al. 2019), LaSOT_{ext} (Fan

et al. 2021) and TNL2K (Wang et al. 2021a), significantly exceeds previous methods such as All-in-one (Zhang et al. 2023), DMTrack-384 (Zhang et al. 2024), JointNLT (Zhou et al. 2023) and QueryNLT (Shao et al. 2024).

LaSOT & LaSOT_{ext}. They are extensions of traditional visual tracking benchmarks (Fan et al. 2019; Li et al. 2017) by adding text labels, focusing on long-term tracking challenges. Furthermore, LaSOT_{ext} also includes many similar distractors, further complicating the tracking task.

As shown in Table 1, GLAD-L384 achieved the highest score in the *AUC* metric, surpassing All-in-one (Zhang et al. 2023) by 4.3%, indicating the effectiveness of our generative fusion paradigm on making full use of high-semantic texts for improvement of target locating. Compared to pure vision models like SeqTrack (Chen et al. 2023b) and ARTTrack (Wei et al. 2023), GLAD-L384 also achieves better performance, which further validates the effectiveness of the template inpainting approach employed by our method.

TNL2K. It is a large-scale benchmark specifically constructed for natural language-guided tracking, consisting of over two thousand video sequences with diverse target categories and fine-grained linguistic annotations. The dataset enables evaluation of the interaction between visual and textual modalities, making it a common choice for studying language-assisted tracking (Wang et al. 2021a).

As shown in Table 1, GLAD-L384 outperforms the recent DMTrack-384 by 0.5% in *AUC* and 0.8% in *P*. Compared to ChatTracker (Sun et al. 2024) which employs multimodal large language models to generate high-quality text annotations for addressing static text limitations, our textual target-context guidance module achieves superior performance by 2.5% in *AUC* and 4.1% in *P*.

OTB99. It is a classical short-term tracking benchmark containing 99 video sequences with manually annotated bounding boxes across a variety of common tracking scenarios. An additional extension, OTB-sentences, provides one natural language description for each sequence, allowing the benchmark to be used in vision-language tracking studies as well (Li et al. 2017).

As shown in Table 1, GLAD-L384 also exhibits leading performance in the *AUC* metric, surpassing All-in-one (Zhang et al. 2023) by 0.4% in *AUC* and 0.2% in *P*. Compared to JointNLT (Zhou

Table 2: Params and MACs analysis of GLAD. All tests were conducted on a RTX 3090 GPU.

Model	Module	Params(M)	MACs(G)
GLAD-B256	Image Encoder	85.6	27.4
	Pooling	17.7	3.4
	Decoding	28.3	13.4
	Head	6.5	1.7
	Total	138.2	41.1
GLAD-L384	Image Encoder	303.1	218.1
	Pooling	18.7	3.6
	Decoding	50.4	52.0
	Head	8.2	4.7
	Total	380.4	259.4
JointNLT	Total	153.0	42.0
MMTrack	Total	176.9	-

et al. 2023) which uses joint visual grounding and tracking framework, we still achieves superior performance by 4.7% in AUC and 5.0% in P, demonstrating the effectiveness of language information and GLAD’s strong capability in utilizing text features.

Table 3: Efficiency analysis of GLAD. All tests were conducted on a RTX 3090 GPU.

Method	Speed (FPS)	LaSOT AUC(%)
JointNLT	39	60.4
TransVLT	36	66.4
VLT _{TT}	48	67.3
MMTrack	45	70.0
GLAD-B256	65	69.5
GLAD-L384	44	76.0

Inference Speed It is a critical factor for practical visual tracking applications, as many scenarios such as autonomous driving, robotics, and surveillance require both accurate and fast target localization. High inference speed ensures that the tracker can respond promptly to dynamic changes in the environment, making it suitable for time-sensitive tasks and large-scale deployment.

To evaluate the efficiency of our method, we conduct a detailed statistical analysis of tracking speed and computational cost. For computational

cost, we reported the parameter count of each module and make a comparison, as shown in Table 2. For tracking speed, we compare GLAD-L384 with several representative approaches in Table 3. The results indicate that GLAD-L384 runs at 44 FPS, which is comparable to VLT_{TT} (Guo et al. 2022) and MMTrack (Zheng et al. 2023). Notably, this high inference speed is achieved while still maintaining competitive accuracy, demonstrating that our generative multi-modal fusion framework effectively balances computational efficiency and tracking performance for real-world applications.

4.3 Extra comparison on traditional visual tracking dataset

Besides, we also evaluate our model on the traditional visual tracking dataset GOT-10k (Huang et al. 2019) to verify the tracking performance in a vision-only scenario. Since GOT-10k contains only visual information without any textual descriptions, it provides an ideal setting to examine whether our generative multimodal fusion paradigm can still contribute to performance improvement when the model relies solely on visual cues. This evaluation also helps determine whether the effectiveness of GLAD stems from its generative modeling ability itself rather than merely from additional language guidance.

As summarized in Table 4. Our GLAD surpasses VLT_{TT} (Guo et al. 2022) by 3.6% on the

Table 4: State-of-the-art comparison on the vision-only dataset GOT-10k. The best two results are shown in **red** and **blue** fonts.

Method	$AO(\%)$	$SR_{0.5}(\%)$	$SR_{0.75}(\%)$
<i>Visual tracking method (vision-only)</i>			
TransT (Chen et al. 2021)	67.1	76.8	60.9
STARK (Yan et al. 2021)	68.8	78.1	64.1
MixFormer (Cui et al. 2022)	71.2	79.9	65.8
MixViT (Cui et al. 2022)	72.7	82.3	70.8
OSStrack-B256 (Ye et al. 2022)	71.0	80.4	68.2
OSStrack-L384 (Ye et al. 2022)	73.7	83.2	70.8
AiATrack (Gao et al. 2022)	69.6	80.0	63.2
SimTrack (Chen et al. 2022)	68.6	78.9	62.4
<i>Vision-language tracking method</i>			
RomTrack (Cai et al. 2023)	72.9	82.9	70.2
VLT _{SCAR} (Guo et al. 2022)	61.4	72.4	52.3
VLT _{TT} (Guo et al. 2022)	69.4	81.1	64.5
GLAD-B256(Ours)	73.0	83.4	69.8
GLAD-L384(Ours)	74.5	84.7	73.1

AO metric and achieves performance comparable to state-of-the-art vision-only trackers such as MixFormer (Cui et al. 2022) and OSStrack (Ye et al. 2022). This demonstrates that even in the absence of textual input, GLAD maintains strong tracking capability and robust visual understanding. These results further validate that the proposed generative paradigm enables the extraction of semantically richer and more discriminative visual representations, ultimately enhancing tracking robustness across different settings.

4.4 Ablation Experiment

To thoroughly evaluate the effectiveness of our proposed method, we conduct comprehensive ablation studies on each major module within the framework. The experiments are carried out on two widely recognized vision-language tracking benchmarks, LaSOT (Fan et al. 2019) and TNL2K (Wang et al. 2021a), which together cover diverse tracking scenarios and varying degrees of textual-visual correspondence. All experiments are performed under the same training and inference configurations to ensure fairness and consistency

in comparison, allowing us to clearly assess the contribution and robustness of each module.

4.4.1 Exploration of Feature Decoding Module

We observed that in current vision-language tracking datasets, the textual descriptions often fail to align precisely with the visual content of the search images, primarily due to the inherent semantic gap between linguistic and visual modalities during the tracking process. This mismatch leads to inaccurate or noisy guidance when textual features are directly fused with the visual representations of search regions, potentially degrading overall performance. To further verify the impact of this issue, we design two variant models for comparative analysis, each aiming to isolate and evaluate the role of textual-visual interaction under different fusion strategies.

Feature Modulation: As shown in the left part of Figure 6a, the template features \mathcal{F}_{tp} and search features \mathcal{F}_{sr} are first concatenated into the combined visual representation \mathcal{F}_v , which is then processed by a simple feature modulation

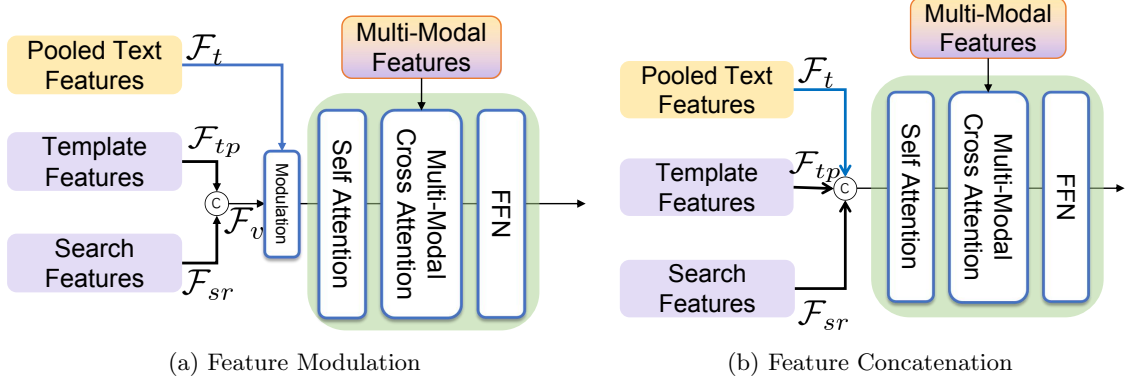


Fig. 6: Two types of text–visual feature fusion methods are illustrated. The template and search features are extracted from the Image Encoder, while the pooled text features are obtained from the Text Encoder in Stable Diffusion, which is equivalent to the Text Encoder used in CLIP. The multi-modal features are produced by the attention pooling module. In the left design, a simple feature modulation is applied to introduce textual information, whereas in the right design, feature concatenation is employed for fusion.

block before being fed into the decoder. This variant aims to inject linguistic cues into the visual pathway through a lightweight modulation mechanism while preserving the original spatial structure of the visual features. The modulation is performed between the visual features \mathcal{F}_v and the textual features \mathcal{F}_t extracted from the text encoder, formulated as:

$$\mathcal{F}_{mod} = \mathcal{F}_v \odot \text{Linear}(\mathcal{F}_t) + \mathcal{F}_v, \quad (23)$$

where \odot denotes the Hadamard product and $\text{Linear}(\cdot)$ represents a learnable linear projection for dimensional alignment.

As shown in Table 5, results of Exp-Decode-M show a decrease δ_1 of 0.8% / 0.6% in AUC and 1.1% / 0.7 % in P on LaSOT / TNL2k separately. **Feature Concatenation:** As shown in the right part of Figure 6b, another variant directly concatenates the template features \mathcal{F}_{tp} and the search features \mathcal{F}_{sr} with the textual features \mathcal{F}_t generated from the text encoder in the generative diffusion module. This design aims to achieve a more explicit multimodal integration by merging all modalities into a unified representation before decoding. The concatenation operation can be formulated as:

$$\mathcal{F}_{cat} = \text{Concat}(\mathcal{F}_{tp}, \mathcal{F}_{sr}, \mathcal{F}_t), \quad (24)$$

where $\text{Concat}(\cdot)$ denotes channel-wise concatenation along the feature dimension. The fused

features are subsequently fed into the decoder for joint reasoning and target localization.

As outlined in Table 5, the results of Exp-Decode-C show a decrease δ_2 of 1.1% / 1.0% in AUC and 1.6 % / 1.2 % in P on LaSOT / TNL2K respectively.

From the two experiments discussed above, it can be concluded that directly incorporating textual features into the decoding process leads to suboptimal results, as the semantic information from language cannot be properly aligned with the visual representation of the search region. This mismatch introduces noise rather than providing meaningful guidance for target localization.

In contrast, leveraging the multi-modal features generated by the proposed Attention Pooling Module enables a more structured and semantically consistent integration of textual cues. Through this mechanism, the text information is effectively embedded into the visual domain, enhancing the quality of the target representation and improving overall tracking performance. These results further verify the effectiveness and superiority of our Attention Pooling Module in bridging the semantic gap between vision and language for robust multimodal tracking.

4.4.2 Utilization of U-Net Features

GLAD leverages features extracted from three intermediate layers of the U-Net architecture, specifically the 5-th, 6-th, and 7-th Transformer

Table 5: Exploration studies. $\delta_1, \delta_2, \dots$, and δ_8 denote the numerical differences compared with GLAD-B256.

Method	LaSOT		TNL2K	
	AUC(%)	P(%)	AUC(%)	P(%)
GLAD-B256	69.5	74.2	59.7	62.2
Exp-Decode-M (δ_1)	68.7 (-0.8)	73.1 (-1.1)	59.1 (-0.6)	61.5 (-0.7)
Exp-Decode-C (δ_2)	68.4 (-1.1)	72.6 (-1.6)	58.7 (-1.0)	61.0 (-1.2)
Exp-UNet-5th (δ_3)	66.5 (-3.0)	68.3 (-5.9)	56.4 (-3.3)	58.7 (-3.5)
Exp-UNet-6th (δ_4)	68.6 (-0.9)	73.2 (-1.0)	59.3 (-0.4)	61.1 (-1.1)
Exp-UNet-7th (δ_5)	67.8 (-1.7)	70.4 (-3.8)	58.5 (-1.2)	60.9 (-1.3)
Exp-UNet-10th (δ_6)	69.9 (+0.4)	75.1 (+0.9)	60.2 (+0.5)	63.5 (+1.3)
Exp-Transformer (δ_7)	67.2 (-2.3)	69.7 (-4.5)	58.3 (-1.4)	61.1 (-1.1)
Exp-SDv3 (δ_8)	70.2 (+0.7)	76.2 (+2.0)	60.9 (+1.2)	62.5 (+0.3)

modules in the contraction path. These submodules correspond to progressively deeper layers responsible for feature extraction, where semantic richness increases while spatial resolution decreases. Therefore, it is reasonable to utilize these layers, as they contain high-level semantic information essential for constructing effective multi-modal representations.

We further analyze the contribution of different U-Net layers through ablation experiments, as summarized in Table 5. When removing the 5-th Transformer module (Exp-UNet-5th, δ_3), the performance drops noticeably, with decreases of 3.0% / 5.9% in AUC and 3.3% / 3.5% in precision on LaSOT / TNL2K, respectively. Removing the 6-th module (Exp-UNet-6th, δ_4) leads to a relatively smaller degradation, resulting in 0.9% / 1.0% AUC drops and 0.4% / 1.1% precision drops on the two datasets. Similarly, excluding the 7-th module (Exp-UNet-7th, δ_5) causes consistent performance decreases of 1.7% / 3.8% in AUC and 1.2% / 1.3% in precision. These results indicate that each selected layer contributes positively to the final performance, and removing any single layer inevitably degrades tracking accuracy.

On the other hand, we also notice that the submodules along the expansion path correspond to the feature reconstruction and fusion stages, where the feature dimensions gradually become shallower. To further explore the potential of these representations, we investigate whether utilizing

features from this stage could provide additional benefits to multi-modal fusion.

Specifically, we conduct an ablation experiment by additionally introducing the 10-th Transformer module from the expansion path. As shown in Exp-UNet-10th of Table 5, a slight improvement of $\delta_3 = 0.4\% / 0.5\%$ in AUC on LaSOT / TNL2K respectively can be observed, indicating that the expansion path still provides useful information for multi-modal feature modeling.

However, it can also be seen from Figure 3b that after the 7-th Transformer module, the spatial resolution of U-Net features increases significantly. Employing such high-resolution features would substantially raise the computational overhead for both the attention pooling and feature decoding modules. Therefore, despite the potential benefits of expansion path features, they are less suitable for a simple and efficient tracking algorithm like ours, where the trade of inference speed and resource utilization are critical considerations.

In addition, we replace the diffusion (U-Net) module as a whole to further analyze its contribution. Specifically, we retain the original model architecture but remove the generative interaction introduced by diffusion. Instead, the text and template are individually encoded into features and fused using a standard transformer module. The fused features are then fed into the same Multi-Modal Decoder, ensuring consistency with the original pipeline.



Fig. 7: Visualizations of Template Inpainting. The first row shows templates before inpainting, the second row shows templates after inpainting, and the third row presents the corresponding text descriptions. The restored templates exhibit clearer textures and richer semantics, facilitating more accurate target representation.

The experimental results are presented in Exp-Transformer of Table 5. As shown, this variant results in a performance degradation, with AUC drops of 2.3% / 4.5% and precision decreases of 1.4% / 1.1% on LaSOT / TNL2K, respectively, indicating that the generative interaction is able to better capture informative feature representations.

4.4.3 Other Diffusion Backbone

To further demonstrate the effectiveness and robustness of the proposed generative fusion paradigm, we additionally explore the use of alternative diffusion backbones. Specifically, we replace the original Stable Diffusion v1.5 model with Stable Diffusion v3 while keeping the rest of the tracking framework unchanged. As shown in Table 5, a consistent performance of $\delta_8 = +0.7\% / +2.0\%$ on LaSOT and $\delta_8 = +1.2\% / +0.3\%$ on TNL2K can be observed across the four benchmarks, indicating that the proposed framework maintains strong tracking performance when adopting a different diffusion backbone.

Besides that, we also believe that fine-tuning the diffusion model on tracking datasets could lead to even better results, as the distribution of the original training data for the diffusion model differs from that of tracking data. However, due to the high computational cost associated with fine-tuning large diffusion models, we have not explored

this direction in the current work. We consider this a promising avenue for future research.

4.5 Analysis of Out-of-Distribution Data

Sometimes, tracking videos may contain out-of-distribution content, such as infrared sequences, which fall outside the typical data distribution of models like SD-v1.5. To evaluate the robustness of our approach in such scenarios, we specifically tested GLAD on these sequences and analyzed its performance. Specifically, we selected all infrared video sequences from the TNL2K test dataset and calculated the AUC. The results are shown in Table 7.

It can be observed that our method achieves a certain performance improvement, indicating that our method demonstrates good generalization ability and can still perform effective tracking on out-of-distribution data such as infrared imagery.

4.6 Analysis of Template Semantics

From Table 1 we can find that our method outperforms most methods which leverage visual grounding to assist in vision-language tracking on several datasets. To further analyze the effectiveness of our method, we will make a analysis from the restoration of semantic perspective of the template since our method is developed from

Table 6: Comparison of tracking performance with and without the template inpainting process. The variant without inpainting excludes the diffusion-guided template enhancement but retains diffusion-based feature extraction.

<i>AUC</i> (%)	LaSOT	TNL2K	OTB99-lang
with template inpainting	69.5	59.7	69.6
without template inpainting	68.4	56.3	68.8

Table 7: AUC of infraed sequences from TNL2K. All tests were conducted on a RTX 3090 GPU.

Method	Infraed Sequence AUC(%)
JointNLT	51.7
VLT _{TT}	48.6
SeqTrack	49.3
GLAD-B256	53.2

the perspective of the restoration of low template semantic.

In our setting, the term low semantic refers to visual inputs that suffer from degraded perceptual quality, resulting in reduced semantic clarity. Such degradation may arise from a wide range of real-world factors, including motion blur caused by rapid movement, insufficient illumination leading to low-contrast scenes, and low-resolution inputs where fine-grained features are underrepresented. Furthermore, environmental influences such as fog, haze, rain streaks, or smog can obscure important visual details, while sensor-level issues—such as high-ISO noise or compression artifacts—introduce distortions that further hinder interpretation. Partial occlusions or visual clutter can also mask key semantic elements. While these images may still contain meaningful content, the presence of such noise and distortion makes semantic extraction more challenging for models, thereby increasing the tracking difficulty for the model.

To facilitate analysis and quantitatively evaluate the improvement, we divide the semantics of the template into two components: the clarity of the tracking target and the relevance to the text description. The former refers to the resolution and detail sharpness of its visual information, while the latter refers to the semantic alignment between the visual features of the image and the linguistic

features of the text. We will discuss the effectiveness of our method from these two perspectives separately.

4.6.1 The Clarity of the Tracking Target

The clarity of the tracking target is highly correlated with the overall performance of a tracking model, as a well-defined and visually detailed target provides more reliable cues for feature extraction and localization. To investigate this relationship, we analyze the influence of template inpainting and further illustrate its impact through visual representations of the inpainting process.

Figure 7 presents several visualizations of the template inpainting results described in the Generative Diffusion Module (Section 3.1). The examples are drawn from LaSOT, OTB99-Lang, and TNL2K datasets. It can be observed that after inpainting, the structural and textural details of the templates are effectively restored, which mitigates issues such as image blur, visual degradation, and ambiguous semantics, ultimately providing a clearer reference for tracking.

To quantitatively assess the contribution of template inpainting, we conduct an additional experiment by re-implementing a variant of our model that excludes the inpainting process but still employs diffusion-based feature extraction. In this variant, only the U-Net component is used to extract template features without diffusion-guided fusion.

As shown in Table 6, the GLAD variant without template inpainting experiences a noticeable performance drop in AUC on LaSOT and an even more significant degradation on TNL2K. These results clearly demonstrate the effectiveness of the template inpainting strategy in enhancing template quality and semantic consistency, thereby validating that diffusion-based fusion of textual and

Table 8: Quantitative statistics on mainstream datasets, including the number and proportion of High / Low-Semantic Frames and High / Low-Semantic Videos, as well as the Average Template Semantics values for each dataset.

Dataset	Concepts	High-Semantic Frame		Low-Semantic Frame		High-Semantic Video		Low-Semantic Video		Average Template Semantics
		Number	Ratio	Number	Ratio	Number	Ratio	Number	Ratio	
LaSOT		15764	46.2%	18352	53.8%	116	41.4%	164	58.6%	24.94
LaSOT _{ext}		8475	47.5%	9358	52.5%	71	47.3%	79	52.7%	24.56
TNL2K		9326	36.7%	16097	63.3%	258	36.9%	442	63.1%	20.32
OTB99-lang		661	46.7%	753	53.3%	20	41.7%	28	58.3%	21.98

visual information plays a crucial role in improving tracking robustness and precision.

4.6.2 Relevance Analysis between Text and Video

Similarly, the relevance between texts and images is also a key factor affecting the performance of the model. To this end, we conducted an analysis on several vision-language tracking datasets. To quantitatively analyze the relevance between text and video on mainstream datasets, including LaSOT (Fan et al. 2019), LaSOT_{ext} (Fan et al. 2021), TNL2K (Wang et al. 2021a) and OTB99-lang (Li et al. 2017).

In typical vision-language tracking settings, the template image and the corresponding textual description are expected to be semantically aligned and mutually complementary, ensuring that the linguistic cue accurately guides the tracker to identify and localize the intended target. Hence, the *degree of semantic alignment* between the template and text can serve as an important indicator for evaluating the *semantic validity, richness, and clarity* of the template representation. A well-aligned pair implies that the visual appearance of the template effectively reflects the semantic meaning expressed in the textual description, which facilitates better cross-modal understanding during tracking.

To quantify this semantic alignment, we employ the CLIP score, a widely recognized metric for measuring image–text correspondence. Specifically, the CLIP (Radford et al. 2021) model jointly encodes visual and linguistic inputs into a shared embedding space, where semantic similarity is represented by the cosine similarity between the image and text embeddings. A higher CLIP score indicates that the template and textual description are more

semantically consistent, suggesting that the template can better convey the intended meaning of the text and thus provide stronger guidance for the tracker. In our study, we use the CLIP score as a quantitative indicator of the semantic coherence between visual and textual modalities.

The formula for calculating the CLIP score is as follows:

$$\text{clip score}(I, T) = \frac{LS \cdot \text{CLIP}(I) \cdot \text{CLIP}(T)}{\|\text{CLIP}(I)\| \cdot \|\text{CLIP}(T)\|}, \quad (25)$$

where LS denotes the *LogitScale*, a learned parameter in the original CLIP model that functions as a temperature coefficient. Here, I represents the image, T represents the text, and $\text{CLIP}(I)$ and $\text{CLIP}(T)$ are the corresponding feature embeddings extracted by the CLIP encoders. The operator “.” indicates the *dot product* between vectors, while $\|\cdot\|$ denotes their *L2 norm*. It is also widely used by image caption models and generative models such as Imagen (Saharia et al. 2022) to evaluate the effectiveness of multi-modal models in matching textual descriptions with corresponding visual content.

After quantifying the semantic correlation between images and textual descriptions, we can further extend this concept to the video-text level to evaluate the overall semantic consistency of videos to measure the global relevance between a video and its corresponding textual description, which reflects how well the textual semantics are preserved across the entire sequence. This assessment helps us better understand whether a tracker benefits from high-quality semantic templates when handling videos with different degrees of visual-textual alignment.

Table 9: CLIP score evaluation under different template degradations.

Video	Raw	Blurring	Occlusion	Darkening	Color Jitter
Clip Score	24.94	21.19	19.86	24.15	23.54

For each video, we first compute the CLIP score for the template image f_0 and then uniformly sample one frame from every 20 frames as the selected search image, denoted as f_{20i} . We compute the CLIP score for each sampled frame to obtain a set of semantic relevance scores:

$$\{S_0, S_{20}, S_{40}, \dots, S_{20i}, \dots\}. \quad (26)$$

This score set represents the semantic correspondence between textual descriptions and video frames, enabling us to analyze the video-level semantic characteristics more effectively. To this end, we define several quantitative metrics as follows.

High / Low-Semantic Frame: For any selected search image f_{20i} ($i > 0$) in a video, if its score S_{20i} is greater than the template score S_0 , it is considered a high-semantic frame; otherwise, it is a low-semantic frame. This distinction helps evaluate the relative semantic adequacy of frames compared to the template.

High / Low-Semantic Video: We calculate the average value \bar{S} of all frame-level scores $\{S_{20i}\}$. If \bar{S} is higher than the template score S_0 , the video is considered a high-semantic video; otherwise, it is regarded as a low-semantic video. This classification reflects the overall semantic relevance between the text and the visual content of the video.

Average Template Semantics: Finally, we compute the average of all template-level scores S_0 across the dataset, which serves as an indicator of the dataset’s overall semantic richness. This metric provides a global reference for comparing the semantic adequacy of templates and understanding their influence on tracking performance.

Based on the above concepts, we conduct a comprehensive statistical analysis on the test splits of LaSOT, TNL2K, OTB99-Lang, and LaSOT_{ext}, as summarized in Table 8. It can be observed that within most videos, the number of low-semantic frames is significantly greater than that of high-semantic ones, indicating that the semantic consistency between the text descriptions and the

visual content is generally weak. Furthermore, the overall proportion of low-semantic videos exceeds that of high-semantic videos across all datasets, revealing that the textual descriptions in current benchmarks often fail to accurately align with or represent the visual targets throughout the entire sequence.

Meanwhile, degradations such as blurring or occlusion further exacerbate the loss of semantic information in the template. To validate this, we conducted an additional experiment: we selected all template images from LaSOT based on our previous CLIP score evaluations and applied four types of degradations to each video—blurring, occlusion, darkening, and color jitter—to create controlled variants. We then recalculated the average CLIP score for each modified video using the same procedure. The results are shown in Table 9. The results are shown below. We observe a consistent decrease in the average CLIP score across all types of degradations, which not only validates our conclusion but also indicates that the CLIP score is a reasonably reliable measure of the overall semantic quality of a video.

This observation implies that directly introducing textual features into the search-region representation may lead to semantic confusion and unstable attention, as the search frames themselves often lack sufficient semantic correspondence with the text. In contrast, the template and the text both serve as descriptions of the same target object — one in visual form and the other in linguistic form. Therefore, enhancing the interaction between template features and textual features allows the model to more effectively consolidate multimodal cues about the target’s appearance and attributes, producing a semantically richer and more consistent target representation. This design philosophy underpins the GLAD framework, which prioritizes generative refinement of the template through text-guided diffusion before performing multimodal fusion. By doing so, GLAD establishes a more reliable target prior, thereby improving the accuracy and robustness of subsequent tracking.

Table 10: Comparison of average template semantics before and after restoration with SD on different datasets.

Dataset	Original Template Semantics	Template Semantics after SD
LaSOT	24.94	25.78
LaSOT-ext	24.56	26.87
TNL2K	20.32	23.09
OTB99-lang	21.98	22.48

In addition, to further quantify the semantic enhancement provided by our approach, we compute the CLIP score for template images before and after template inpainting using Stable Diffusion (SD) and compare the average template semantics across datasets. The results, shown in Table 10, demonstrate a consistent improvement in the post-restoration CLIP scores. This indicates that our diffusion-based inpainting effectively enhances the semantic expressiveness of templates, bringing them closer to the text descriptions and improving the overall multimodal alignment. Consequently, these refined templates contribute to more reliable visual-textual associations, which are crucial for achieving stable and accurate tracking performance in vision-language scenarios.

5 Conclusion

In this paper, we have proposed a new vision-language tracking method GLAD. It's based on the novel generative multi-modal fusion paradigm and comprises the Generative Diffusion Module and the cascaded Multi-Modal Decoder. Textual information is firstly fused with template features for semantic restoration. Search features are then interacted with the generated multi-modal features for semantic enhancement. The experiments have demonstrated that our method effectively restores low-semantic templates and enhances tracking performance. Besides, we also present a comprehensive analysis of template semantics to further confirm the effectiveness and theoretical reliability of our method. As a result, our GLAD achieves excellent performance in both accuracy and inference speed. We hope GLAD can provide a new option for the tracking community in the future.

Acknowledgement.

This work is supported by the National Natural Science Foundation of China (Grant No. 62402211) and the Natural Science Foundation of Jiangsu Province (Grant No. BK20241248).

Conflict of interest statement.

There is no specific conflict of interest statement with this manuscript

Compliance of ethical standard statement.

There is no specific compliance of ethical standard statement with this manuscript

Informed consent.

There is no specific informed consent with this manuscript

Funding Information.

This work is supported by the National Natural Science Foundation of China (Grant No. 62402211) and the Natural Science Foundation of Jiangsu Province (Grant No. BK20241248).

Data Availability.

This manuscript develops its method based on the publicly available datasets: GOT-10k (Huang et al. 2019), LaSOT (Fan et al. 2019), OTB99-lang (Li et al. 2017), TNL2K (Wang et al. 2021a), TrackingNet (Muller et al. 2018), RefCOCOg (Mao et al. 2016). There is no specific associated data with this manuscript and the code included in this study are available upon request by contact with the corresponding author.

References

Bertinetto L, Valmadre J, Golodetz S, et al (2016)
Staple: Complementary learners for real-time

tracking. In: CVPR. IEEE Computer Society, pp 1401–1409

Bhat G, Johnander J, Danelljan M, et al (2018) Unveiling the power of deep tracking. In: ECCV (2), Lecture Notes in Computer Science, vol 11206. Springer, pp 493–509

Bhat G, Danelljan M, Gool LV, et al (2019) Learning discriminative model prediction for tracking. In: Proceedings of the IEEE/CVF international conference on computer vision, pp 6182–6191

Brown T, Mann B, Ryder N, et al (2020) Language models are few-shot learners. *Advances in neural information processing systems* 33:1877–1901

Cai Y, Liu J, Tang J, et al (2023) Robust object modeling for visual tracking. In: Proceedings of the IEEE/CVF International Conference on Computer Vision (ICCV), pp 9589–9600

Chen B, Li P, Bai L, et al (2022) Backbone is all your need: A simplified architecture for visual object tracking. In: ECCV (22), Lecture Notes in Computer Science, vol 13682. Springer, pp 375–392

Chen S, Sun P, Song Y, et al (2023a) Diffusiondet: Diffusion model for object detection. In: Proceedings of the IEEE/CVF International Conference on Computer Vision, pp 19830–19843

Chen X, Yan B, Zhu J, et al (2021) Transformer tracking. In: Proceedings of the IEEE/CVF conference on computer vision and pattern recognition, pp 8126–8135

Chen X, Peng H, Wang D, et al (2023b) Seqtrack: Sequence to sequence learning for visual object tracking. In: CVPR. IEEE, pp 14572–14581

Chen X, Kang B, Geng W, et al (2025) Sutrack: Towards simple and unified single object tracking. In: Proceedings of the AAAI Conference on Artificial Intelligence, pp 2239–2247

Cheng Z, Zhu F, Zhang XY, et al (2025) Breaking the limits of reliable prediction via generated data. *International Journal of Computer Vision* 133(3):1195–1221

Cui Y, Jiang C, Wang L, et al (2022) Mixformer: End-to-end tracking with iterative mixed attention. In: Proceedings of the IEEE/CVF conference on computer vision and pattern recognition, pp 13608–13618

Cui Y, Song T, Wu G, et al (2023) Mixformerv2: Efficient fully transformer tracking. *Advances in neural information processing systems* 36:58736–58751

Danelljan M, Bhat G, Khan FS, et al (2019) ATOM: accurate tracking by overlap maximization. In: CVPR. Computer Vision Foundation / IEEE, pp 4660–4669

Devlin J, Chang MW, Lee K, et al (2018) Bert: Pre-training of deep bidirectional transformers for language understanding. *arXiv preprint arXiv:181004805*

Dhariwal P, Nichol A (2021) Diffusion models beat gans on image synthesis. *Advances in neural information processing systems* 34:8780–8794

Dosovitskiy A, Beyer L, Kolesnikov A, et al (2020) An image is worth 16x16 words: Transformers for image recognition at scale. *arXiv preprint arXiv:201011929*

Fan H, Lin L, Yang F, et al (2019) Lasot: A high-quality benchmark for large-scale single object tracking. In: Proceedings of the IEEE/CVF conference on computer vision and pattern recognition, pp 5374–5383

Fan H, Bai H, Lin L, et al (2021) Lasot: A high-quality large-scale single object tracking benchmark. *International Journal of Computer Vision* 129:439–461

Feng Q, Ablavsky V, Bai Q, et al (2020) Real-time visual object tracking with natural language description. In: Proceedings of the IEEE/CVF Winter Conference on Applications of Computer Vision, pp 700–709

Feng Q, Ablavsky V, Bai Q, et al (2021) Siamese natural language tracker: Tracking by natural language descriptions with siamese trackers. In: Proceedings of the IEEE/CVF conference on computer vision and pattern recognition, pp

Gao S, Zhou C, Ma C, et al (2022) Aiatrack: Attention in attention for transformer visual tracking. In: ECCV (22), Lecture Notes in Computer Science, vol 13682. Springer, pp 146–164

Ge SR, Cao J, He R (2025) Improving object detection models via llm-based training data synthesis. International Journal of Computer Vision pp 1–16

Glorot X, Bengio Y (2010) Understanding the difficulty of training deep feedforward neural networks. In: Proceedings of the thirteenth international conference on artificial intelligence and statistics, JMLR Workshop and Conference Proceedings, pp 249–256

Guo M, Zhang Z, Fan H, et al (2022) Divert more attention to vision-language tracking. Advances in Neural Information Processing Systems 35:4446–4460

He K, Zhang X, Ren S, et al (2016) Deep residual learning for image recognition. In: Proceedings of the IEEE conference on computer vision and pattern recognition, pp 770–778

He K, Chen X, Xie S, et al (2022) Masked autoencoders are scalable vision learners. In: CVPR. IEEE, pp 15979–15988

Ho J, Jain A, Abbeel P (2020) Denoising diffusion probabilistic models. Advances in neural information processing systems 33:6840–6851

Huang B, Lian D, Luo W, et al (2021) Look before you leap: Learning landmark features for one-stage visual grounding. In: Proceedings of the IEEE/CVF conference on computer vision and pattern recognition, pp 16888–16897

Huang L, Zhao X, Huang K (2019) Got-10k: A large high-diversity benchmark for generic object tracking in the wild. IEEE transactions on pattern analysis and machine intelligence 43(5):1562–1577

Karras T, Aittala M, Aila T, et al (2022) Elucidating the design space of diffusion-based generative models. Advances in Neural Information Processing Systems 35:26565–26577

Kingma DP, Welling M (2013) Auto-encoding variational bayes. arXiv preprint arXiv:13126114

Li X, Ren Y, Jin X, et al (2025) Diffusion models for image restoration and enhancement: a comprehensive survey. International Journal of Computer Vision pp 1–31

Li Y, Yu J, Cai Z, et al (2022) Cross-modal target retrieval for tracking by natural language. In: Proceedings of the IEEE/CVF Conference on Computer Vision and Pattern Recognition, pp 4931–4940

Li Z, Tao R, Gavves E, et al (2017) Tracking by natural language specification. In: Proceedings of the IEEE conference on computer vision and pattern recognition, pp 6495–6503

Loshchilov I, Hutter F (2017) Decoupled weight decay regularization. arXiv preprint arXiv:171105101

Lugmayr A, Danelljan M, Romero A, et al (2022) Repaint: Inpainting using denoising diffusion probabilistic models. In: CVPR. IEEE, pp 11451–11461

Luo S, Tan Y, Patil S, et al (2023) Lcm-lora: A universal stable-diffusion acceleration module. arXiv preprint arXiv:231105556

Ma D, Wu X (2023) Tracking by natural language specification with long short-term context decoupling. In: Proceedings of the IEEE/CVF International Conference on Computer Vision, pp 14012–14021

Mao J, Huang J, Toshev A, et al (2016) Generation and comprehension of unambiguous object descriptions. In: CVPR. IEEE Computer Society, pp 11–20

Muller M, Bibi A, Giancola S, et al (2018) Trackingnet: A large-scale dataset and benchmark for object tracking in the wild. In: Proceedings of the European conference on computer vision (ECCV), pp 300–317

Pnvr K, Singh B, Ghosh P, et al (2023) Ld-znet: A latent diffusion approach for text-based image segmentation. In: Proceedings of the IEEE/CVF International Conference on Computer Vision, pp 4157–4168

Quan W, Chen J, Liu Y, et al (2024) Deep learning-based image and video inpainting: A survey. *International Journal of Computer Vision* 132(7):2367–2400

Radford A, Kim JW, Hallacy C, et al (2021) Learning transferable visual models from natural language supervision. In: International conference on machine learning, PMLR, pp 8748–8763

Rajbhandari S, Rasley J, Ruwase O, et al (2020) Zero: Memory optimizations toward training trillion parameter models. In: SC20: International Conference for High Performance Computing, Networking, Storage and Analysis, IEEE, pp 1–16

Rasley J, Rajbhandari S, Ruwase O, et al (2020) Deepspeed: System optimizations enable training deep learning models with over 100 billion parameters. In: Proceedings of the 26th ACM SIGKDD International Conference on Knowledge Discovery & Data Mining, pp 3505–3506

Rassin R, Ravfogel S, Goldberg Y (2022) Dalle-2 is seeing double: Flaws in word-to-concept mapping in text2image models. arXiv preprint arXiv:221010606

Rezende DJ, Mohamed S, Wierstra D (2014) Stochastic backpropagation and approximate inference in deep generative models. In: International conference on machine learning, PMLR, pp 1278–1286

Rombach R, Blattmann A, Lorenz D, et al (2022) High-resolution image synthesis with latent diffusion models. In: Proceedings of the IEEE/CVF conference on computer vision and pattern recognition, pp 10684–10695

Ronneberger O, Fischer P, Brox T (2015) U-net: Convolutional networks for biomedical image segmentation. In: Medical image computing and computer-assisted intervention–MICCAI 2015: 18th international conference, Munich, Germany, October 5–9, 2015, proceedings, part III 18, Springer, pp 234–241

Russakovsky O, Deng J, Su H, et al (2015) Imagenet large scale visual recognition challenge. *International journal of computer vision* 115(3):211–252

Saharia C, Chan W, Saxena S, et al (2022) Photorealistic text-to-image diffusion models with deep language understanding. *Advances in neural information processing systems* 35:36479–36494

Shao Y, He S, Ye Q, et al (2024) Context-aware integration of language and visual references for natural language tracking. In: Proceedings of the IEEE/CVF Conference on Computer Vision and Pattern Recognition, pp 19208–19217

Sohl-Dickstein J, Weiss E, Maheswaranathan N, et al (2015) Deep unsupervised learning using nonequilibrium thermodynamics. In: International conference on machine learning, PMLR, pp 2256–2265

Song Y, Ermon S (2019) Generative modeling by estimating gradients of the data distribution. *Advances in neural information processing systems* 32

Song Y, Ermon S (2020) Improved techniques for training score-based generative models. *Advances in neural information processing systems* 33:12438–12448

Song Y, Ma C, Wu X, et al (2018) VITAL: visual tracking via adversarial learning. In: CVPR. Computer Vision Foundation / IEEE Computer Society, pp 8990–8999

Song Y, Sohl-Dickstein J, Kingma DP, et al (2020) Score-based generative modeling through stochastic differential equations. arXiv preprint arXiv:201113456

Song Y, Durkan C, Murray I, et al (2021) Maximum likelihood training of score-based diffusion models. *Advances in neural information processing systems* 34:1415–1428

Song Y, Dhariwal P, Chen M, et al (2023) Consistency models. arXiv preprint arXiv:230301469

Sun Y, Yu F, Chen S, et al (2024) Chattracker: Enhancing visual tracking performance via chatting with multimodal large language model. In: NeurIPS

Vaswani A, Shazeer N, Parmar N, et al (2017) Attention is all you need. Advances in neural information processing systems 30

Wang X, Shu X, Zhang Z, et al (2021a) Towards more flexible and accurate object tracking with natural language: Algorithms and benchmark. In: Proceedings of the IEEE/CVF conference on computer vision and pattern recognition, pp 13763–13773

Wang Z, Zhao H, Li Y, et al (2021b) Do different tracking tasks require different appearance models? In: NeurIPS, pp 726–738

Wei X, Bai Y, Zheng Y, et al (2023) Autoregressive visual tracking. In: Proceedings of the IEEE/CVF Conference on Computer Vision and Pattern Recognition, pp 9697–9706

Yan B, Peng H, Fu J, et al (2021) Learning spatio-temporal transformer for visual tracking. In: ICCV. IEEE, pp 10428–10437

Yang Z, Gong B, Wang L, et al (2019) A fast and accurate one-stage approach to visual grounding. In: Proceedings of the IEEE/CVF international conference on computer vision, pp 4683–4693

Yang Z, Kumar T, Chen T, et al (2020) Grounding-tracking-integration. IEEE Transactions on Circuits and Systems for Video Technology 31(9):3433–3443

Ye B, Chang H, Ma B, et al (2022) Joint feature learning and relation modeling for tracking: A one-stream framework. In: European conference on computer vision, Springer, pp 341–357

Zhang C, Sun X, Yang Y, et al (2023) All in one: Exploring unified vision-language tracking with multi-modal alignment. In: Proceedings of the 31st ACM International Conference on Multimedia, pp 5552–5561

Zhang G, Zhong B, Liang Q, et al (2024) Diffusion mask-driven visual-language tracking. In: IJCAI.

ijcai.org, pp 1652–1660

Zhang Z, Peng H, Fu J, et al (2020) Ocean: Object-aware anchor-free tracking. In: Computer Vision–ECCV 2020: 16th European Conference, Glasgow, UK, August 23–28, 2020, Proceedings, Part XXI 16, Springer, pp 771–787

Zhao B, Yin W, Meng L, et al (2020) Layout2image: Image generation from layout. International journal of computer vision 128(10):2418–2435

Zhao H, Wang X, Wang D, et al (2023) Transformer vision-language tracking via proxy token guided cross-modal fusion. Pattern Recognition Letters 168:10–16

Zheng Y, Zhong B, Liang Q, et al (2023) Toward unified token learning for vision-language tracking. IEEE Transactions on Circuits and Systems for Video Technology 34(4):2125–2135

Zhou L, Zhou Z, Mao K, et al (2023) Joint visual grounding and tracking with natural language specification. In: Proceedings of the IEEE/CVF conference on computer vision and pattern recognition, pp 23151–23160

Zhou X, Wang D, Krähenbühl P (2019) Objects as points. CoRR abs/1904.07850